

Characterization of Type-I ELM Induced Filaments in ASDEX Upgrade

A. Schmid¹, A. Herrmann¹, A. Kirk², J. Neuhauser¹, S. Günter¹, H.W. Müller¹,
M. Maraschek¹, V. Rohde¹ and the ASDEX Upgrade Team.

¹ *Max-Planck-Institut für Plasmaphysik, EURATOM-IPP Association, Garching, Germany*

² *EURATOM/UKAEA Fusion Association, Culham Science Centre, Abingdon, UK*

Introduction

Next step fusion devices such as ITER are based on a H-Mode scenario which is characterised by the formation of a transport barrier near the plasma edge. Periodic relaxations of this transport barrier lead to a fast expulsion of energy and particles from the plasma edge, so called ELMs (edge localized modes). The amount of energy released by an ELM increases with confinement, i.e. with the size of the experiment, so that high ELM losses are expected for ITER and other next step fusion devices [1]. The energy release in ELMs is burst like, with coherent substructures, so called filaments, within the ELM. Filaments rotate poloidally/toroidally and move radially towards the low field side wall, carrying some fraction of the ELM energy loss towards the wall. They are extended along field lines and have an extent of a few centimeters perpendicular to the field lines. They deposit their energy locally and might lead to largely enhanced erosion of wall materials in future fusion devices.

For an extrapolation to future devices, it is necessary to understand the basic mechanisms behind filaments and their role in radial heat and particle transport, requiring detailed knowledge of the filament dynamics, density and temperature.

Diagnostic setup

Langmuir probes are an important tool to measure filament properties, as they provide localized measurements (small pin size) and can be run at high sampling rates (Isat mode, 2 MHz). On ASDEX Upgrade, filament studies have successfully been carried out using Langmuir probes on a reciprocating midplane manipulator [2]. These probes clearly show filamentary structures passing by, but are not suited for measuring filament velocities because of the small distance between the Langmuir pins. As the probe size on the midplane manipulator is limited by feedthroughs, we have installed a new in-vessel probe at the magnetic low-field side, where ELM induced filaments are expected to have their maximum amplitude. This dedicated filament probe [3] consists of several Langmuir pins at suitable distances (≈ 10 cm) and a magnetic pick-up coil in the center. The probe features a magnetic drive, which allows a radial motion of the probe from a safe position behind the limiters to a position in front of the leading ICRH limiters [3]. It allows to investigate the filament structure and dynamics, in particular filament rotation (by time delay measurements), size (by peak width analysis) and temperature (in combination with IR thermography [4]). It is positioned at the ASDEX Upgrade low field side such that it is connected to the midplane manipulator along a magnetic field line. This allows the measurement along one filament with both filament and midplane manipulator probe. Here,

we have used a dual magnetic probe, which consists of two 3D coilsets that measure all three components of the magnetic field at two different radial positions.

Filament Rotation Velocities

Filaments are assumed to be field aligned structures, i.e., their inclination angle is about equal to the local field line inclination angle, which is between 7° and 14° for typical ASDEX Upgrade discharges ($q_{95} = 3 - 6$). They move radially and rotate poloidally and/or toroidally. Because of the field aligned structure, however, only the cross field rotation velocity can be uniquely determined. If poloidal or toroidal velocities are quoted in the following, it is assumed that the cross field motion is caused by filament rotation in the respective direction only.

The insert in figure 1 shows a front view of the filament probe as seen from the plasma. The probe has 4 pins, which are hit subsequently as filaments move past the probe.

The filament velocity can be inferred from the pin distance perpendicular to the magnetic field and the arrival times of the filament at the Langmuir pins. Figure 1 shows the time series of the 4 Langmuir signals, shifted in y according to the distance of the pins perpendicular to the local magnetic field.

The Langmuir probes are operated in Isat mode, so that filaments show up as prominent peaks in fig. 1. Peaks belonging to one filament moving with constant velocity can be connected via straight lines. Rotation velocities can be calculated from the slope of these lines. Typical poloidal rotation velocities are between 2000 m/s and 4000 m/s and are directed poloidally downwards. Alternatively, this would correspond to a toroidal rotation velocity of 10-20 km/s in the co-current direction, which is a similar order to the pedestal rotation velocity before the ELM. The velocity of the filaments seems to decrease within an ELM. From an analysis of the peak width together with the velocities derived above, the filament size perpendicular to the field line can be calculated to be 20-30 mm.

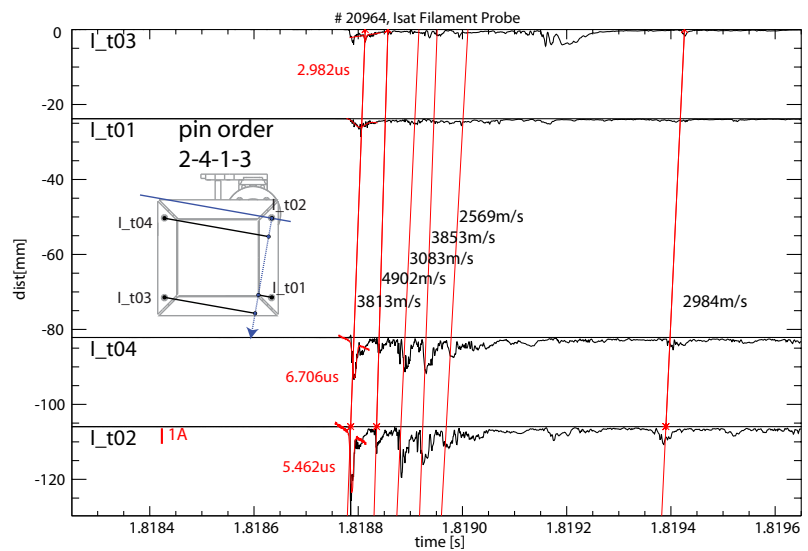


Figure 1: Filament (blue line) moving in poloidal direction (inlay). The 4 pins are hit subsequently, giving pronounced peaks in the Isat measurement. The slope of lines that connect peaks belonging to one filament gives the rotation velocity, the peak width gives the size of the filament.

$\mathbf{E} \times \mathbf{B}$ Drift as a Model for Radial Filament Propagation

Due to the radially varying toroidal magnetic field B_{tor} , filaments become polarized by $\nabla \mathbf{B}$ drift. The polarization leads to a current $\parallel \mathbf{B}$ because of a partial short circuit at the intersection with the wall. The residual voltage drop across the ohmic sheath resistance causes a poloidal electric field E_{pol} , which drives the radial motion via $\mathbf{E} \times \mathbf{B}$ drift [5].

As the $\nabla \mathbf{B}$ drift happens all along the filament, the current inside the filament should increase towards the target plates. The maximum current that can flow in such a filament is, however, limited by the ion saturation current, which can be measured with Langmuir probes and is in the order of 15 A/cm^2 .

Simulation of the Magnetic Signature

Combining measurements from filament probe and midplane manipulator gives a total of 7 magnetic coils to measure the magnetic signature of a filament.

A program has been written to calculate the magnetic signature of a moving filament. The code takes size and position of the magnetic coils into account and assumes a Gaussian shaped current density distribution. Parameters such as filament size, velocity, current density and distribution, position of the filament can be adjusted to fit the measured signal. These parameters are not independent from each other: A faster filament gives a higher amplitude with lower peak width, a larger distance reduces the amplitude. The Langmuir measurements were used to fix velocity and size in the calculations. The influence of the current distribution and the ratio of radial to poloidal velocity was investigated by parameter variation and by matching the calculations to the measurements:

Current distribution. Bipolar and unipolar current distributions were investigated. Bipolar currents give a more complex signal (e.g. with additional minima), whereas unipolar

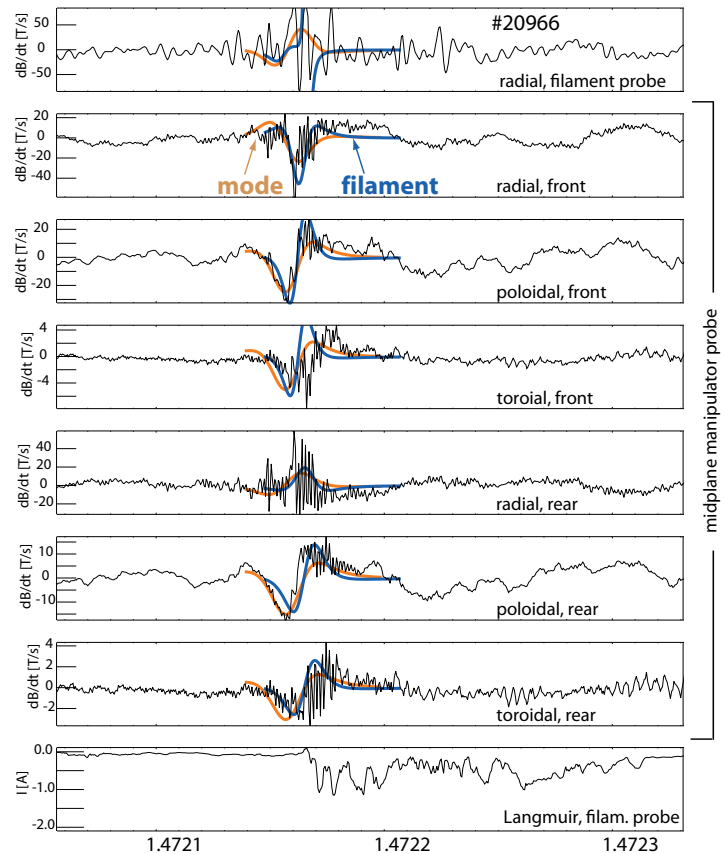


Figure 2: Comparison of the calculated magnetic signature with the signal measured by the magnetic coil inside the filament probe and 2 coilsets which measure all 3 field components at 2 different radial positions.

currents give a much broader, simpler signal, which would require remarkably faster or smaller filaments (compared to the values inferred from the Langmuir probe measurements). The qualitative agreement is better for bipolar currents.

Velocity ratio v_r/v_{pol} . 3 different cases have been investigated: structures moving with a velocity ratio $v_r/v_{pol} = 1 : 0.2$ (i.e. a mostly radial motion), with $v_r \approx v_{pol}$, and structures with mostly poloidal velocity $v_r \ll v_{pol}$. The first 2 cases correspond to filaments travelling through the SOL, the latter case corresponds to magnetic modes rotating close to the pedestal, inside the separatrix. Fig. 2 shows a comparison of a best fit derived from a rotating filament as well as from a rotating mode. From qualitative arguments, no clear preference can be found. Quantitative analysis reveals, however, that running filaments (i.e. the first 2 cases) together with bipolar current distributions would require a current of 200-300 A per filament, corresponding to a current density of 170-230 A/cm², which is much higher than the measured ion saturation current density of 15 A/cm².

If the magnetic signal would be caused by radially moving filaments, one would furthermore expect, that about one half of the filaments passes below the probe, whereas the other half passes above the probe. This should change the sign of the magnetic signature, as the polarization direction is always the same for $\nabla\mathbf{B}$ polarized filaments. However, such a change could not be observed: the magnetic data suggest that virtually all filaments pass the probe at the same side (co-current rotation). This indicates, that the magnetic signature on ASDEX Upgrade is by some part dominated by short-lived magnetic structures inside the separatrix. In order to give a final answer to that question, one would require a measurement of the radial velocity of filaments.

Summary

Several measurements of the propagation velocity of Type-I ELM induced filaments have been carried out using Langmuir probes and magnetic pick-up coils. Combined measurements have been used to predict the current inside a filament. The analysis suggests that modes rotating in the co-current direction inside the separatrix play an important role in the formation of filaments. Measurements of the radial propagation velocity will be carried out in 2007 to reduce the available parameter space of the calculations and to answer the question of the origin of the magnetic signature during Type-I ELMs.

References

- [1] A. Herrmann et al., J. Nucl. Mater., **313-316**, 759 (2003)
- [2] A. Kirk et al., Plasma Phys. Controlled Fusion, **47**, 995 (2005)
- [3] A. Schmid et al., Review of Scientific Instruments **78**, 053502 (2007)
- [4] A. Herrmann et al., J. Nucl. Mater., **363-365**, 528 (2007)
- [5] S. I. Krasheninnikov, Physics Letters A, **283**, 368 (2001)